Transient and Steady Flow from Subsurface Line Sources at Constant Hydraulic Head in Anisotropic Soil

Christiaan Dirksen

ABSTRACT

WATER content and pressure head distributions were measured during transient and steady flows from four equally spaced line sources maintained at constant hydraulic head in very fine sand in a large laboratory model. Theory and experiment agreed reasonably well. The major differences were a much reduced upward flow and an increased lateral flow below the sources in the experiments. This, and considerations concerning differences in horizontal versus vertical flow between sources, indicated that the soil column exhibited varying degrees of anisotropy, with the hydraulic conductivity being greater horizontally than vertically. After initial wetting, water contents changed little until the wetting fronts reached the bottom. Then the water began to accumulate from the bottom upward. Differences in infiltration rates between sources were predominantly determined by conditions around the sources and were reflected in rates of advance of the wetting fronts, rather than the water content in the regions of uniform flow farther below the sources. Subsequent drainage of the sand provided data for determining the hydraulic conductivity functions and the soil water characteristics. At the same water content, the hydraulic conductivity during wetting was only about half of that during drying.

INTRODUCTION

Subsurface irrigation has a number of attractive features that enhance energy and water conservation. For instance, subsurface systems can often be operated continuously at low pressures, representing savings in pipe sizes and energy consumption. Reducing evaporation and tailoring the water supply to the needs of the crop offer potential for significant water savings. On the other hand, subsurface irrigation systems are generally designed with little or no overlap and salt will tend to accumulate at the perimeter of the wetted areas, particularly above the source. More complete discussions of these and other technological and managerial aspects of subsurface irrigation can be found in McNamara (1970) and other papers and references in the Proceedings of the National Irrigation Symposium.

To design and manage subsurface irrigation systems properly, the flow characteristics must be understood and predicted for various conditions. Recently, a number of analytical and numerical solutions have become available that provide basic understanding of unsaturated soil water flow problems. Those pertaining particularly to line sources are Raats (1970, 1977), Philip (1971, 1972), Thomas, Kruse and Duke (1974), and Lomen and Warrick (1974). They are analytical solutions of linearized equations for steady flow obtained by assuming an exponential relationship between pressure head and hydraulic conductivity.

Few experimental studies are available by which these solutions can be tested. Thomas et al. (1976) compared calculated and measured pressure heads for steady infiltration from buried line sources in two soils. They found generally good agreement in the flow region above the line sources, but the comparison directly beneath the line sources was poor. They suggest that the latter may be due to inadequate simulation of the lower boundary condition. Thomas et al. (1977) used the same experimental setup to determine the influence of root water uptake by two crops on the pressure head distributions. The effect was largest in the area above the laterals, where the pressure heads were much lower than without plants. Merrill et al. (1978) compared theoretical and experimental pressure heads for a point source at the surface of a heterogeneous soil column and found best agreement at low flow rates. Bresler et al. (1971) found generally good agreement between experimental and theoretical water content distributions for transient flow from an array of surface point sources, which approximated a line source. The theoretical results were obtained numerically rather than by an analytical solution. Snyder et al. (1973) measured the water content in the first 15 cm of soil as a function of the distance from the line sources buried 10 cm deep in a fine sand amended with clay or shredded pine bark.

This paper presents experimental water content and water potential data obtained during transient and steady flow from four subsurface line sources in very fine sand. The data are analyzed to obtain insight into the qualitative aspects of flow from buried line sources. A comparison with steady flow theory and other observations suggest that the soil column exhibited varying degrees of anisotropy of hydraulic conductivity.

EXPERIMENTAL

The experiments were carried out in a laboratory model with a two-dimensional automatic gamma ray attenuation scanner described elsewhere (Dirksen and Huber, 1978). The model was packed by hand, in 0.03- to 0.05-m-thick layers at a time, with very

Article was submitted for publication in September 1977; reviewed and approved for publication by the Soil and Water Division of ASAE in December 1977.

Contribution from the U.S. Salinity Laboratory, SEA, USDA, 4500 Glenwood Dr., Riverside, CA.

The author is CHRISTIAAN DIRKSEN, Soil Scientist, U.S. Salinity Laboratory, Riverside, CA.

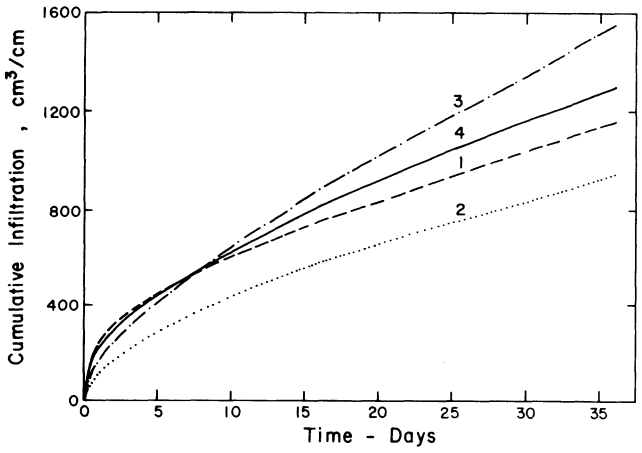

FIG. 1 Cumulative infiltration of four line sources at constant head for 36-day period.

fine sand smaller than 0.25 mm. The thickness and depth of the sand pack were 0.102 m and 1.056 m, respectively, and the total length was 3.15 m, without partitions. During the packing, four 6.4 mm OD porous ceramic tubes were installed across the pack at depth $z_0 = 0.395$ m from the surface, with lateral distances between sources of $a = 0.775$ m. After gamma attenuation data were obtained for each grid point through the dry sand, water was supplied through the ceramic tubes at a constant positive head of 0.71 m water inside the ceramic tubes. Wetting fronts were traced on the glass walls at various times until they reached the bottom of the sand pack.

Water was supplied for 36 days. After that, starting about two days later, the sand was drained for seven days by maintaining a suction of 1.28 m water in the filter candles at the bottom of the sand pack. All this time, gamma attenuation measurements were regularly made. The vertical spacing between grid points was 0.089 m, the horizontal spacing was either 0.102 or 0.152 m. Tensiometric measurements were also made at 22 locations, spread unevenly over the flow field of two of the four sources. The tensiometers consisted of thin ceramic disks epoxied in the end of 1/4 NPT male tubing connectors. Once installed firmly against the sand pack, they performed satisfactorily without spring loading. The tensiometers were read automatically, by means of a hydraulic switching valve and a pressure transducer (Kistler, Redmond, Washington, Model 311D).* This pressure transducer covers the entire tensiometer range of pressure heads with an accuracy of about 1 mm water. During the wetting phase, the overall accuracy of most of the tensiometric data approached that of the transducer, but during the draining phase the accuracy decreased somewhat, mainly due to problems with the hydraulic switching valve. All data were recorded on paper tape.

RESULTS

Fig. 1 shows the cumulative amounts of infiltration for each of the four line sources for the entire wetting period. Source #2 had consistently the lowest amount.

*The company name is included for the benefit of the reader and does not imply any endorsement or preferential treatment of the product listed by the USDA.

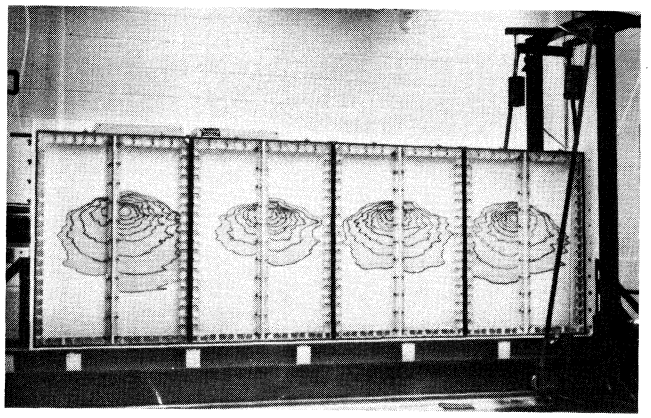

FIG. 2 Wetting fronts of four line sources, traced after 0.25, 0.5, 1.0, 1.5, 2.5, 4.0, 8.25, 19.75 and 45.0 h of wetting at constant head.

It trailed the other three sources by 31 percent at the cross-over point, which occurred after about 1 week. Source #1 had initially the highest rate of infiltration, but after about three days its rates were only slightly larger than those of source #2. Source #3 was initially the slowest of the three fastest and its wetting front was the last of the three to reach the bottom of the column. Yet it did not slow down as much, and its final rate of infiltration was exactly double that of source #2. Source #4 was intermediate to sources #3 and #1.

Fig. 2 is a photograph of the model after 45 h of wetting. The wetting fronts were traced on the glass windows after 0.25, 0.5, 1.0, 1.5, 2.5, 4, 8.25, 19.75, and 45 h of wetting. The sizes and shapes of the wetted areas of the various line sources show quite a variation. There is also appreciable asymmetry between the halves of the flow fields of three of the line sources. During the early stages, the wetting fronts generally advanced farther horizontally than downward. After about two days, the time when the photograph was taken, the vertical advance began to overtake the horizontal advance. The wetting fronts were often more rectangular than semicircular. Because there were no partitions between the sources, they began to influence each other before the wetting fronts reached the bottom of the sand pack. At that stage, the wetting fronts became more or less horizontal.

Fig. 3 shows contours of equal volumetric water content $\Theta(cm^3/cm^3)$ for the entire flow field after 10 days. At that time the wetting front had reached the bottom over the full width associated with source #4 and over approximately half the width of sources #1 and #3, but the wetting front of source #2 was still about 0.15 m away from the bottom. Most of the water contents fell between 0.12 and 0.09 m. The wetting fronts were much sharper at the bottom than at the top. Contours for $\Theta < 0.09$ are omitted at the bot-

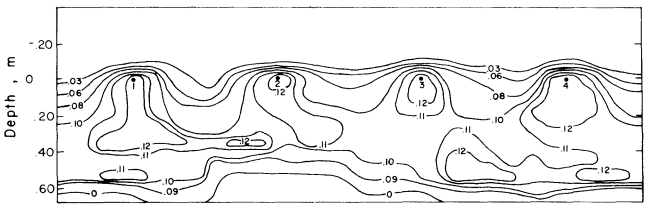

FIG. 3 Contours of measured equal water content after 10 days of wetting.

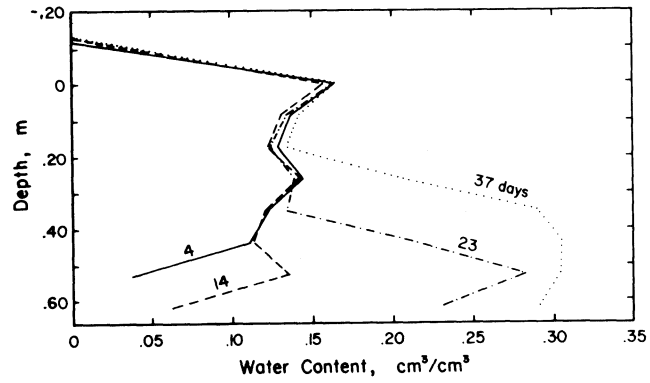

FIG. 4 Water content profile of vertical plane x = 0.025 m of source #1, after 4, 14, 23, and 37 days.

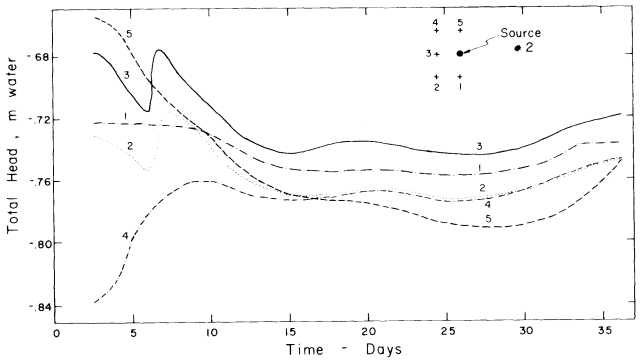

FIG. 5 Total hydraulic heads at five points around source #2, as indicated. H = 0 for h = 0 at z = 0.

tom except for the $\Theta = 0$ contour. It shows the farthest possible extent of the wetting front, but may have been located even closer to the $\Theta = 0.09$ contour. At the top, the wetting front is not indicated, but it followed closely the $\Theta = 0.03$ contour. The regions of high water contents around the sources, indicated only by the $\Theta = 0.12$ contour, differ in size and shape. The water contents around the sources were highest during the first day of wetting. For instance, the highest water content close to source #1 was measured after 3.5 h at $\Theta = 0.210$ cm³/cm³. After a few days, it stabilized at about $\Theta = 0.160$ cm³/cm³. The magnitude of this variation in water content decreased with increasing distance from the source.

Except for these initial higher values, the water contents around the line sources changed very little. This is illustrated by Fig. 4, which shows water content profiles of the vertical plane x = 0.025 m to the right of source #1 at days 4, 14, 23, and 37, respectively. The scan at day 37 was taken about 16 h after the water supply was stopped. These data show that the water just drained through the soil column to advance the wetting front until it reached the bottom. After that the water began to accumulate from the bottom upward.

Most of the tensiometric measurements were made in the area between sources #1 and #2. Fig. 5 shows the total head, H, in meters of water, at five points of a 0.076 m rectangular grid around source #2 (indicated in the figure) from day 3 through day 36. The reference for H is H = 0 for a pressure head h = 0 at the depth of the line sources z = 0, where H = h - z, z positive downward. The original data showed some variations due to the closeness of the measuring points to the line source and the unavoidable disturbances caused by refilling the water supply. In view of the large time scale and the small total head scale, the curves are slightly smoothed representations of the original data. Only points #2 and #3 show a shift in H of about +0.04 m water around day 7. Point #5 showed initially the highest potential. Obviously, the effect of the initially higher water contents around the source remained longer at this point than at the other points. Fig. 6 shows the total head, H, at four positions in the vertical plane a distance x = 0.144 m to the left of line source #1 at depths, z, below the source of 0, 0.153, 0.305, and 0.508 m, respectively.

The drainage was mainly a one-dimensional process. It is sufficiently characterized by Fig. 7, which shows the average water content profile for the area of source #1 after about 20, 90, and 145 h, and Fig. 8, which shows the water potential profiles at the same times, measured with the same tensiometers as in Fig. 6. The drainage occurred much faster than the wetting. After 6 days, most of the water in excess of that corresponding to the imposed pressure head of -1.28 m water at the bottom had been removed.

DISCUSSION

Measured water contents and pressure heads at various positions and times were assembled into one plot. This resulted in very distinct wetting and drying soil-water characteristics, with little scatter in the data points and a pronounced hysteresis effect (Fig. 9). At the dry end, the two curves merge at about $\Theta = 0.04$ cm³/cm³ and h = -1.50 m. The air-entry value for the drying curve is close to h = -0.60 m,

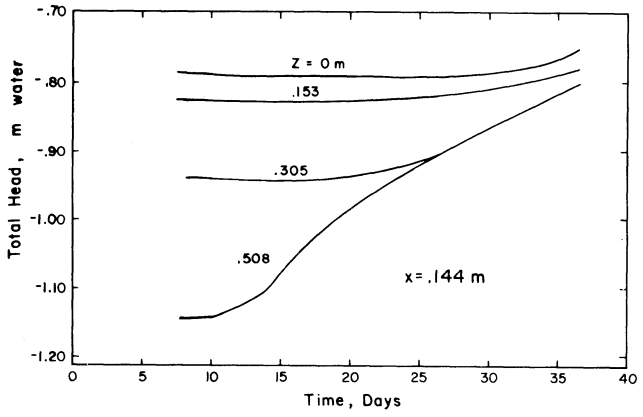

FIG. 6 Total hydraulic heads for source #1 at x = 0.144 m and z = 0, 0.153, 0.305, and 0.508 m. H = 0 for h = 0 at z = 0.

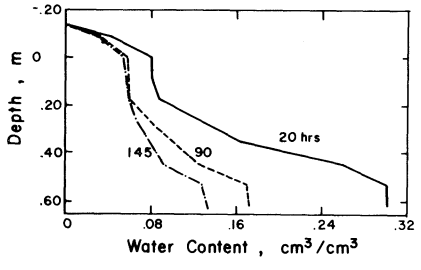

FIG. 7 Average water content profiles in area of source #1, after 20, 90, and 145 h of drainage.

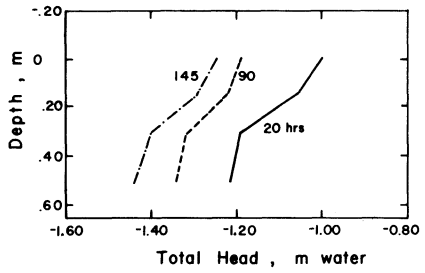

FIG. 8 Total hydraulic head profiles at same locations as in Fig. 6, at same times as in Fig. 7.

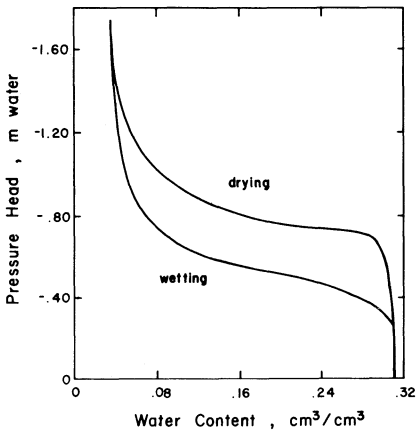

FIG. 9 Composite wetting and drying soil water characteristics.

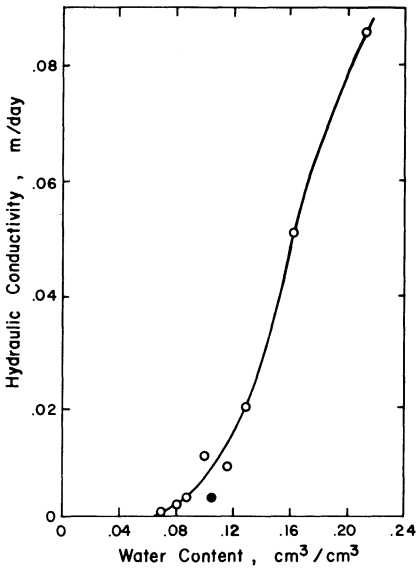

FIG. 10 Calculated hydraulic conductivities vs. observed water contents during drainage. • is dervied from wetting data.

while the wetting curve approaches saturation at about h = -0.25 m.

The data of Fig. 7 and 8 were used to calculate hydraulic conductivities during drainage by averaging fluxes and hydraulic gradients at a number of depths. The results are given in Fig. 10 as hydraulic conductivity as a function of observed average water contents. Also, the average pressure heads observed during drainage and the derived hydraulic conductivities were subjected to an exponential regression. The result is shown in Fig. 11 on a semilog scale. The regression coefficient $R^2 = 0.936$ and the slope $a = 16.8\ m^{-1}$. Similarly, the k(Θ) relationship of Fig. 10 was transformed into an exponential k(h) relationship for wetting via the wetting characteristic in Fig. 9. This is also plotted in Fig. 11. The regression coefficient of this exponential regression $R^2 = 0.974$ and the slope $a = 15.8\ m^{-1}$. Thus the exponential fit is even better for wetting than that for drying. Because the wetting characteristic indicates that the soil becomes saturated around h = -0.25 m water, which projects the saturated hydraulic conductivity at $k_{sat} = 5.7 \times 10^{-5}$ m/s, the exponential relationship between hydraulic conductivity and pressure head during wetting can be represented by

$$k = 5.7 \times 10^{-5} \exp 15.8\,(h + 0.25)\ m/s,\ h < -0.25\ m\ water \quad [1]$$

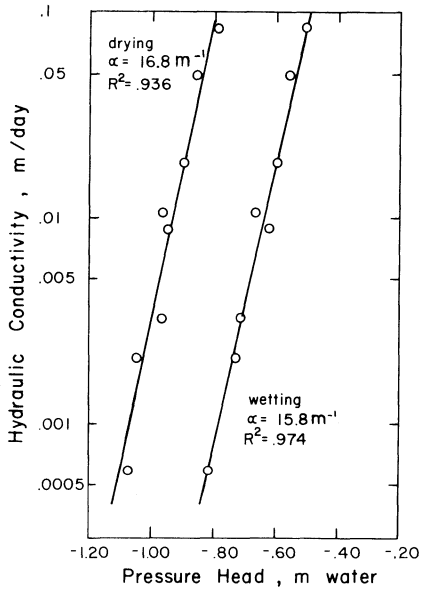

FIG. 11 exponential k[h] relationships for wetting [$a = 15.8\ m^{-1}$, $R^2 = 0.974$] and for drying [$a = 16.8\ m^{-1}$, $R^2 = 0.936$].

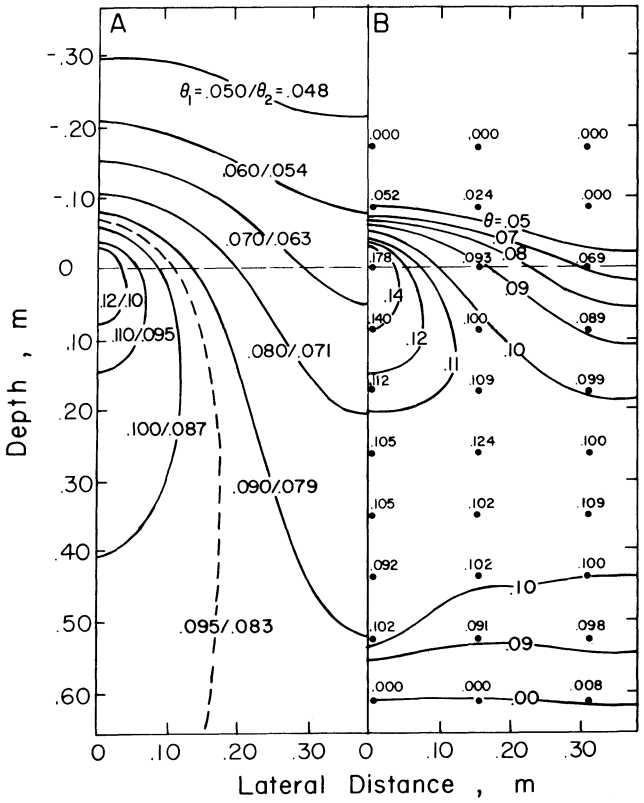

FIG. 12A Theoretical contours of equal water content for steady flow from line source in infinite strip of soil, with a = 0.775 m, $a = 15.8\ m^{-1}$, $k_0 = 2.94 \times 10^{-3}$ m/s, and wetting soil water characteristic of Fig. 9. Θ_1 labels for Q = 0.050 cm³/m,s; Θ_2 labels for Q = 0.025 cm³/m,s. 12B Observed water contents and derived contours of left side of source #3 after 10 days of wetting.

With the value $a = 15.8\ m^{-1}$ in equation [1], matrix flux potentials $\varnothing$ were calculated for steady flow from a line source in an infinite strip according to Thomas et al. (1974, equations [13] to [15]):

$$\phi = (Q/a\alpha)\left\{1 + \sum_{n=1}^{\infty} 2/\mu_n) \exp\left[(\alpha z/2)(1-\mu_n)\right] \cos\left[(2n\pi x)/a\right]\right\} \quad z \geqslant 0 \quad [2]$$

$$\phi = (Q/\alpha a)\left\{\exp(\alpha z) + \sum_{n=1}^{\infty} (2/\mu_n) \exp\left[(\alpha z/2)(1+\mu_n)\right] \cos\left[(2n\pi x)/a\right]\right\} \quad z \leqslant 0 \quad [3]$$

$$\mu_n = \left\{1 + \left[(4n\pi/a\alpha)\right]^2\right\}^{1/2} \quad [4]$$

In these equations, a is the lateral spacing and Q is the source strength per unit length of line source. The matric flux potentials were converted to pressure heads according to Thomas et al. (1974, equation [23]):

$$h = \left[\ln \phi - \ln k_o/\alpha\right]/\alpha \quad [5]$$

where $k_o = 2.94 \times 10^{-3}$ m/s is the hydraulic conductivity for h = 0 according to equation [1]. The pressure heads, in turn, were converted to water contents via the wetting soil water characteristic in Fig. 9. Fig. 12A shows contours of equal volumetric water content Θ thus calculated for a = 0.775 m, which corresponds to a rather large value of $A = \alpha a/2 = 6.12$ for the dimensionless lateral spacing used by Thomas, et al. (1974). Within a limited range of source strengths, the contour pattern is nearly identical; only the labels need to be changed. Fig. 12A gives labels Θ_1 and Θ_2 for source strengths Q of 0.050 and 0.025 cm^3/m, s, or average infiltration rates of 5.6 and 2.8 mm/day, respectively. The first is equal to the constant rate observed for source #3 from day 8 to day 12, the second is 10 percent higher than the rate observed for source #2 at day 10. Thus this twofold range covers the range of observed infiltration rates for Fig. 3. These contours can be compared with Fig. 3, because, as will be argued next, it represents essentially steady-state conditions.

On day 10 (Fig. 3), most wetting fronts were approaching the bottom of the column and Fig. 6 shows that from day 8 to day 10, in the vertical plane at distance x = 0.144 m to the right of source #1, the hydraulic gradient between z = 0.508 m was exactly 1.00 m water/m. Also, the tensiometric data showed little difference in the lateral direction. Already at depth z = 0.0153 m below source #1 on day 10, the differences between H at x = 0.144, 0.212, and 0.373 m were only 1, 5, and 17 mm water, respectively. This suggests that the bottom part of the flow region was a "transition zone" through which the water was just draining toward the bottom of the column by gravity. At day 10, the wetting fronts had advanced far enough that the depth of column had little influence on the flow system. The same is indicated by water contents in the lower region of the column. They are for the most part within experimental error of an average water content of $\Theta = 0.105\ cm^3/cm^3$. Even for source #2 this average water content appears to be established, although the wetting front is still about 0.15 m away from the bottom. The only exception is the region of source #4 and part of source #3 near the bottom where the wetting front had reached the bottom and some water had begun to accumulate.

Whereas the water contents in the bottom of the soil column were all essentially the same, the rates and amounts of infiltration from the sources were not. Expressed as depth of water over the surface area per source, the rates at day 10 were 3.3, 2.5, 5.6, and 4.4 mm/day, and the total amounts of infiltration were about 75, 55, 82, and 79 mm for sources #1 through #4, respectively. The lower amount of total infiltration for source #2 is reflected in the much smaller advance of its wetting front. Near the wetting front, there is little influence of the surrounding sources on source #2. The flux of source #3 was more than twice as large as that of source #2, while the hydraulic gradients above the wetting fronts were probably all approximately unity. This indicates that the fluxes and water contents equilibrated in a range where relatively small water content changes caused relatively large changes in hydraulic conductivity. This agrees with Fig. 10, which shows a relatively sharp increase in $dk/d\Theta$ around $\Theta = 0.10\ cm^3/cm^3$. The magnitude of the fluxes appears to be mainly determined by the conditions near the source and any differences were reflected more in the rate of advance of the wetting fronts than in water contents. These, then, are conditions approaching a steady state, which allow Fig. 3 to be compared with the theoretical solution of Fig. 12A.

In comparing Figs. 3 and 12A, one must realize that the theoretical contours were drawn with a high degree of accuracy, whereas Fig. 3 is based on interpolation of a limited number of water contents with an experimental error of about $\pm 0.003\ cm^3/cm^3$ and influenced by irregularities in bulk density, etc. For a better comparison, Fig. 12B gives on the same scale the original observed water contents and the derived contours for the left side of source #3 in Fig. 3. The contours were obtained by linear interpolation except close to the source, since the theoretical results show a relatively fast decrease of Θ in that region. A comparison of Fig. 12B with 12A (labels Θ_1) shows clearly the main qualitative differences between theory and experiment: the observed upward flow of water was much smaller and the lateral flow was larger than theory predicts. Very little upward wetting occurred beyond that shown in Fig. 2. Even after 36 days, the wetting front extended to only about 0.13 m above the sources. The increased lateral flow caused the higher, more uniform water contents below the line sources.

Quantitatively, the agreement between theory and experiment below the source is quite good. The theoretical water contents also become more uniform with depth. Below z = 0.40 m, they vary less than 0.01 cm^3/cm^3. The average value is about $\Theta = 0.095\ cm^3/cm^3$, which is about 0.01 cm^3/cm^3 less than the observed average value. Above that depth, the average value of Θ remains about the same, but the variation in the horizontal direction increases. For the smaller source strength, these average water contents differ

about 0.02 cm^3/cm^3 (see contour 0.095/0.083).

The qualitative differences between theory and experiment are accentuated by the observation that agreement is the worst "above and away from the laterals," which is exactly where Thomas et al. (1976) found the best agreement for their pressure head distributions. Actually, they based an entire design procedure on the theoretical pressure heads in this upper corner. An obvious explanation for this discrepancy would be that layering of the sand pack caused the hydraulic conductivity to be larger in the horizontal than in the vertical direction. There is additional evidence for such anisotropy.

First, during the first 2 days the wetting fronts advanced further horizontally than vertically. In homogeneous and isotropic soil, wetting fronts are elongated in the downward direction unless the effect of gravity is negligible. In that case, they are circular. Then there are the differences in size and shape of the wetted areas between the four line sources in Figs. 2 and 3. These differences could have been caused by differences in permeability of the ceramic of the line sources, although the ceramic tubes were of uniform, high permeability. The water was delivered under the same constant pressure head of +0.71 m water. The permeability most likely decreased some with time and may have caused the initial decrease in water content near the sources. Any significant decrease in permeability of the line sources should have resulted in a significant decrease in water potential around the source, and this was not observed, at least not for source #2 after day 2. Fig. 5 shows that at 0.076 m below source #2, the total head did not vary by more than 0.04 m water, starting at day 3. (No data are available for the first 2 days.)

There were also differences between halves of the flow field of the same source. This may have been caused by variations in contact with the sand around the perimeter of the ceramic tubes. However, the tubes were all similarly installed during packing in a way that allowed some settling, which most likely was insignificant in this sand. A better explanation appears to be that the rate of infiltration depended on the number and size of horizontal fingers in the wetting fronts. For instance, the most fingered wetting fronts are displayed by the fastest wetting, right-hand side of source #1, with immediately adjacent to it the relatively smooth (especially close to the source) wetting fronts of the slowest wetting, left-hand side of source #2. The relatively high water contents measured 0.36 m below source #1 appear also to have been caused by a layering effect that enhanced horizontal flow by impeding vertical flow. The effect extends half way into the flow field of source #2 (Fig. 3). As for source #1, this resulted in bell-shaped contours very similar to those observed by Thomas et al. (1976) for pressure heads, suggesting that they may have experienced a similar problem with layering. All this leads to the conclusion that nonuniform layering caused the hydraulic conductivity to be nonuniformly greater in the horizontal than in the vertical direction.

During the first 4 h of wetting, the ratio of horizontal to vertical advance of the wetting fronts ranged from about 1.2 for source #1 to 1.8 for source #3. Because gravity is relatively unimportant during the very early stages of any form of infiltration (Philip, 1969), these ratios are a first approximation of the ratio of horizontal to vertical hydraulic conductivities. It would be interesting if the theory could be extended to predict the flow patterns in Fig. 3 based on a ratio of horizontal to vertical hydraulic conductivities of such a small magnitude.

The dynamics of the accumulation process after the wetting fronts reached the bottom are represented by the tensiometric data in Fig. 6. At $z = 0.508$ m, the total head H started to increase due to the accumulation at day 10. It continued to increase until the end of the wetting period, when it reached the value $H = -0.797$ m of water, which corresponds with a pressure head $h = -0.289$ m. This means that at day 36, the bottom of the soil at $z = 0.711$ m was still at $h = -0.086$ m. This agrees with the fact that despite the column becoming saturated at the bottom (see Fig. 9), free drainage was not obtained from the filter candles without suction until the end of the wetting period. At $z = 0.305$ m, the first detectable deviation of H from its steady value occurred on day 15. After day 29, the total head difference between the two tensiometers at $z = 0.508$ m and $z = 0.305$ m never exceeded 1 mm water. This means that the pressure below $z = 0.305$ m became essentially hydrostatic. The flow associated with the continuing wetting below this depth was accommodated by a near zero vertical hydraulic gradient. While the soil was wetting up below $z = 0.305$ m, the hydraulic gradient between $z = 0.153$ m and $z = 0.305$ m was at first only about 0.77 m/m and gradually decreased with time after day 20. The lateral hydraulic gradients, which at day 10 were already small at $z = 0.153$ m, became even smaller with time.

The tensiometric data in Fig. 6, described earlier in connection with the "transition zone," permit an estimate of the vertical hydraulic conductivity during wetting. That is, if we assume that all the flow from the line source contributed toward advancing the wetting front and none to wetting up the soil above the wetting front, then the hydraulic conductivity of the transition zone is equal to the rate of infiltration, because the hydraulic gradient is unity. The rate of infiltration for source #1 from day 8 to day 10 was about 0.0034 m/day. Since some flow may have gone into wetting up soil closer to the source or may have been diverted horizontally toward source #2, this flux is an upper limit for that in the "transition zone." Also, the average water content $\Theta = 0.105$ cm^3/cm^3 mentioned earlier is a lower limit because the span between the two tensiometers included part of the wetter region below source #1. Therefore, an estimate for the hydraulic conductivity of $k = 0.0034$ m/day during wetting at a water content $\Theta = 0.105$ cm^3/cm^3 would be an upper limit. This value is indicated in Fig. 10 by the solid dot. It is at least two times smaller than the hydraulic conductivity derived from the drainage data for the same water content. Calculations between $z = 0.153$ and $z = 0.305$ m showed even more pronounced differences.

Similar qualitative differences between wetting and drying were observed by Poulovassilis and Tzimas (1975). Others have found the $k(\Theta)$ relationship nonhysteretic. (See e.g., Rogers and Klute, 1971) Poulovassilis (1969) distinguished two ways in which hysteresis can affect hydraulic conductivity: differences

in the radii of the pores containing water and differences in the coordinates of those pores. The two ways may have opposite effects and cancel each other. Here, both wetting and drying data were obtained with the same tensiometers at the same positions. The tensiometric data during drainage were not quite as accurate as those during wetting, and some simplifying assumptions were used in both cases. Although the data definitely indicate that at the same water content, the hydraulic conductivity was at least two times higher during drying than during wetting, one cannot consider the hysteresis of $k(\Theta)$ to be shown conclusively, because the data are too few and they were not checked independently.

CONCLUSIONS

Just before the wetting fronts of the four line sources at constant hydraulic head reached the bottom of the column, more or less steady rates of infiltration were observed. They ranged from 80 to 190 cm^3/m, which, for the lateral spacing used, corresponds to 2.5 to 5.9 mm/day. In this range, and possibly beyond that to the practical limit of 10 mm/day, the rate of infiltration appeared to depend mainly on the conditions in the immediate vicinity of the source. Toward the bottom, water contents were uniform and relatively independent of the flux. They adjusted to each other in a range where small changes in water content can accommodate relatively large changes in hydraulic conductivity. Differences in infiltration rates were reflected more in the rate of wetting front advance than in the water content.

The steady flow theory agreed fairly well with the experimental results. The observed discrepancies of considerable less upward flow and more lateral flow can be explained by a larger hydraulic conductivity horizontally than vertically. Additional evidence for this anisotropy was discussed. It remains to be seen whether the observed discrepancies can be predicted theoretically with the rather small ratios of k suggested by the initial wetting fronts. If so, discrepancies between theory and experiment as a result of the assumptions involved in the theory can easily be overshadowed by the effect of inhomogeneity or anisotropy of the soil. This sand column was expected to be isotropic; most natural soils have pronounced layering. In such soils, one can expect even more lateral flow and less flow toward the soil surface. Both represent potential economic benefits for subsurface irrigation systems in terms of larger lateral spacing and reduced evaporation and salt accumulation at the soil surface.

References

1 Bresler, E., J. Heller, N. Diner, I. Ben-Asher, A. Brandt, and D. Goldberg. 1971. Infiltration from a trickle source: II. Experimental data and theoretical predictions. Soil Sci. Soc. Amer. Proc. 35:683-689.

2 Dirksen, C., and M. J. Huber. 1978. Soil-water flow model with two-dimensional automatic gamma-ray attenuation scanner. Water Resources Research. 14:611-614.

3 Lomen, D. O., and A. W. Warrick. 1974. Time-dependent linearized infiltration. II. Line sources. Soil Sci. Soc. Amer. Proc. 38:568-572.

4 McNamara, J. B. 1970. Subirrigation — The basis of tomorrow's agriculture. Proc. Nat'l Irrigation Symposium, Univ. of Nebraska, Lincoln, NE, pp. C1-C14.

5 Merrill, S. D., P. A. C. Raats, and C. Dirksen. 1978. Laterally confined flow from a point source at the surface of an inhomogeneous soil column. Soil Sci. Soc. Am. J:42(6), Nov.-Dec.

6 Philip, J. R. 1969. Theory of infiltration. In Advances in Hydroscience, 5:215-296. Academic Press, New York.

7 Philip, J. R. 1971. General theorem on steady infiltration from surface sources, with application to point and line sources. Soil Sci. Soc. Amer. Proc. 35:867-871.

8 Philip, J. R. 1972. Steady infiltration from buried, surface, and perched point and line sources in heterogeneous soils: I. Analysis. Soil Sci. Soc. Amer. Proc. 36:268-273.

9 Poulovassilis, A. 1969. The effect of hysteresis of pore-water on the hydraulic conductivity. J. Soil Sci. 20:52-56.

10 Poulovassilis, A. and E. Tzimas. 1975. The hysteresis in the relationship between hydraulic conductivity and soil water content. Soil Sci. 120:327-331.

11 Raats, P. A. C. 1970. Steady infiltration from line sources and furrows. Soil Sci. Soc. Amer. Proc. 34:709-714.

12 Raats, P. A. C. 1977. Laterally confined, steady flows of water from sources and to sinks in unsaturated soils. Soil Sci. Soc. Amer. J. 41:294-304.

13 Rogers, J. S., and A. Klute. 1971. The hydraulic conductivity-water content relationship during nonsteady flow through a sand column. Soil Sci. Soc. Amer. Proc. 35:695-700.

14 Snyder, G. H., E. O. Burt, J. S. Rogers, and K. L. Campbell. 1973. Theory and experimentation for turf irrigation from multiple subsurface point sources. Soil and Crop Sci. Soc. of Florida Proc. 33:37-41.

15 Thomas, A. W., H. R. Duke, and E. G. Kruse. 1977. Capillary potential distributions in root zones using subsurface irrigation. TRANSACTIONS of the ASAE 20:62-67.

16 Thomas, A. W., H. R. Duke, D. W. Zachmann, and E. G. Kruse. 1976. Comparisons of calculated and measured capillary potentials from line sources. Soil Sci. Soc. Amer. J. 40:10-14.

17 Thomas, A. W., E. G. Kruse, and H. R. Duke. 1974. Steady infiltration from line sources buried in soil. TRANSACTIONS of the ASAE 17:125-128.